

Revisiting fits to $B^0 \rightarrow D^{*-}\ell^+\nu_\ell$ to measure $|V_{cb}|$ with novel methods and preliminary LQCD data at non-zero recoil

Daniel Ferlewicz,¹ Phillip Urquijo,¹ and Eiasa Waheed²

¹*School of Physics, University of Melbourne, Australia*

²*High Energy Accelerator Research Organization (KEK), Japan*

We present a study of fits to exclusive $B^0 \rightarrow D^{*-}\ell^+\nu_\ell$ measurements for the determination of the Cabbibo-Kobayashi-Maskawa matrix element magnitude $|V_{cb}|$, based on the most recent Belle untagged measurement. Results are obtained with the Caprini-Lellouch-Neubert (CLN) and Boyd-Grinstein-Lebed (BGL) form factor parametrizations, with and without the inclusion of preliminary Lattice QCD measurements of form factors at non-zero hadronic recoil from the JLQCD collaboration. The CLN and BGL fits are also studied in different scenarios with reduced theoretical assumptions, and at higher order expansions, respectively. To avoid bias from high systematic uncertainty correlations we use a toy MC approach with a Cholesky decomposition of the covariance matrix. We find that $\mathcal{F}(1)\eta_{EW}|V_{cb}| = (35.2 \pm 0.2 \pm 0.8) \times 10^{-3}$ for CLN and $(34.9 \pm 0.3 \pm 1.0) \times 10^{-3}$ for BGL(1,0,2) without input from Lattice QCD. The errors quoted correspond to statistical and systematic uncertainties, respectively. We find no evidence to support lepton flavor dependence on the measurement of $|V_{cb}|$ but find some tension in the results associated with the ratio of form factors R_1 . We show how input from JLQCD allows for well-defined fit results with reduced model dependence in CLN and BGL. The results obtained using preliminary values are consistent between different orders of parametrizations, ultimately providing a method for a model-independent exclusive measurement of $|V_{cb}|$. Using preliminary inputs from the JLQCD collaboration, $\mathcal{F}(1)\eta_{EW}|V_{cb}|$ is found to be approximately $(34.9 \pm 0.2 \pm 0.9) \times 10^{-3}$ in BGL(1,1,2).

I. INTRODUCTION

The Cabbibo-Kobayashi-Maskawa matrix element $|V_{cb}|$ is a fundamental parameter of the Standard Model, describing the weak decay of b -quarks and must be measured. A long-standing discrepancy between inclusive and exclusive decay mode determinations limits our present understanding of this parameter. The world-average value from combined inclusive results is based on measurements of semileptonic B meson decays, $B \rightarrow X_c \ell \nu$, where X_c denotes all possible hadronic states in the $b \rightarrow c \ell \nu$ transition. The inclusive value is reported to be [1]

$$|V_{cb}| = (42.2 \pm 0.8) \times 10^{-3}. \quad (1)$$

The exclusive measurements are determined from both $B^0 \rightarrow D^{*-}\ell^+\nu_\ell$ and $B^0 \rightarrow D^-\ell^+\nu_\ell$ decays. The results from $B^0 \rightarrow D^{*-}\ell^+\nu_\ell$ decay,

$$|V_{cb}| = (38.4 \pm 0.7 \pm 0.5 \pm 1.0) \times 10^{-3}, \quad (2)$$

using $\mathcal{F}(1) = 0.904 \pm 0.012$, and those from $B^0 \rightarrow D^-\ell^+\nu_\ell$ decays,

$$|V_{cb}| = (39.5 \pm 0.9) \times 10^{-3}, \quad (3)$$

using $\mathcal{G}(1) = 1.05 \pm 0.004 \pm 0.008$, are significantly lower than that from the inclusive approach [1]. These modes must be studied in further detail to understand from where the discrepancies could be originating.

The exclusive value of $|V_{cb}|$ is typically extracted from fits to yields of $B^0 \rightarrow D^{*-}\ell^+\nu_\ell$ decays as a function of the kinematic observables: the hadronic recoil, w , and three angular variables $\cos \theta_\ell$, $\cos \theta_\nu$ and χ . Hadronic

recoil is defined as

$$w = \frac{m_{B^0}^2 + m_{D^{*\pm}}^2 - q^2}{2m_{B^0}m_{D^{*\pm}}}, \quad (4)$$

where q^2 is the invariant mass squared of the lepton-neutrino system and m_{B^0} and $m_{D^{*\pm}}$ are the B^0 and $D^{*\pm}$ meson masses, respectively. θ_ℓ (θ_ν) is the angle between the direction of the lepton (D^0 meson) and the direction opposite to the B meson in the W boson (D^* meson) rest frame. χ is the angle between the planes formed by the decays of the W and D^* mesons in the rest frame of the B meson. The differential decay rate as a function of the hadronic recoil is given by

$$\frac{d\Gamma}{dw} = (\text{Phase space}) |V_{cb}|^2 (\eta_{EW} \mathcal{F}(w))^2, \quad (5)$$

where $\eta_{EW} = 1.0066$ is an electroweak correction for the semileptonic decay [2] and $\mathcal{F}(w)$ combines the form factors relevant to the decay as a function of w . Fits to the observables in this decay are used to extrapolate measurements to the zero-recoil point, $w = 1$, using values of form factors obtained from unquenched Lattice Quantum Chromodynamic (LQCD) calculations. Measurements of $|V_{cb}|$ from $B^0 \rightarrow D^{*-}\ell^+\nu_\ell$ decays have typically used two different parametrizations for fits in order to calculate form factors; one by Caprini, Lellouch and Neubert (CLN) [3] and another by Boyd, Grinstein, and Lebed (BGL) [4]. Both the CLN and BGL parametrizations are built from the same foundations of operator product expansions, where analytic properties of form factors can also introduce some constraints. The CLN parametrization makes use of Heavy Quark Effective Theory (HQET) relations and its constraints on the $B^0 \rightarrow D^{*-}\ell^+\nu_\ell$ form

factors to reduce the number of independent free parameters with respect to BGL.

The 2019 untagged Belle measurement of $|V_{cb}|$ [5] measures $B^0 \rightarrow D^{*-}\ell^+\nu_\ell$ yields in 10 bins for each of the observables and utilizes a forward folding approach to fit to the CLN and BGL parametrizations, measuring $\mathcal{F}(1)\eta_{EW}|V_{cb}| = (35.06 \pm 0.15 \pm 0.56) \times 10^{-3}$ and $(34.93 \pm 0.23 \pm 0.59) \times 10^{-3}$, respectively. These results showed consistency between the two parametrizations at a given order in the BGL expansion, in contrast to the results based on a preliminary measurement with tagged Belle data [6], as covered by Refs. [7, 8] and others. Both fit studies acknowledge that the observed discrepancy may have been a feature of the tagged data set. The Belle results are consistent with a four-dimensional analysis from BABAR [9], with $\mathcal{F}(1)\eta_{EW}|V_{cb}| = (35.02 \pm 0.77) \times 10^{-3}$ in CLN and $(34.98 \pm 0.82) \times 10^{-3}$ in BGL, where the BGL parametrization also required truncation. However, various studies [10, 11] have shown that the choice of configuration in CLN and BGL and the implementation of systematic uncertainties has an effect on the measured value of $|V_{cb}|$ and the relevant form factors in exclusive measurements. In this study, we will use both the CLN parametrization and the BGL parametrization in fits to further explore the Belle results, checking for consistency in measurements between parametrizations and to constrain new phenomena that may violate lepton flavor universality. By including additional data from preliminary LQCD calculations, we seek to model the data at higher orders in the CLN and BGL parametrizations that are therefore far less model dependent.

This paper is organized as follows. Section II provides a brief summary of the conventions used in this analysis. In Section III, we discuss a method in which systematic uncertainties can be taken into account when correlations between observed measurements are very high (predominantly from scale uncertainties). In Section IV we test the compatibility of results from electron and muon decay modes. Sections V and VI explore fits to the CLN and BGL parametrizations with more degrees of freedom, followed by the incorporation of additional LQCD data in Section VII. The results are then summarized and discussed in Section VIII.

II. FORM FACTOR PARAMETRIZATION

In the standard CLN parametrization, the form factor h_{A_1} and the form factor ratios R_1 and R_2 are defined in terms of the free parameters ρ^2 , $R_1(1)$ and $R_2(1)$ as

$$\begin{aligned} h_{A_1}(w) &= h_{A_1}(1) \left[1 - 8\rho^2 z(w) + (53\rho^2 - 15)z(w)^2 \right. \\ &\quad \left. - (231\rho^2 - 91)z(w)^3 \right], \\ R_1(w) &= R_1(1) - 0.12(w-1) + 0.05(w-1)^2, \\ R_2(w) &= R_2(1) + 0.11(w-1) - 0.06(w-1)^2, \end{aligned} \quad (6)$$

where $z(w) = \frac{(\sqrt{w+1}-\sqrt{2})}{(\sqrt{w+1}+\sqrt{2})}$. These are related to Eq. 5 by:

$$\begin{aligned} \mathcal{F}^2(w) &= h_{A_1}^2(w) \left(1 + 4 \frac{w}{w+1} \frac{1-2wr+r^2}{(1-r^2)} \right)^{-1} \times \\ &\quad \left[2 \frac{1-2wr+r^2}{(1-r)^2} \left(1 + R_1^2(w) \frac{w-1}{w+1} \right) \right. \\ &\quad \left. + (1 + (1-R_2(w)) \frac{w-1}{1-r})^2 \right], \end{aligned} \quad (7)$$

where $r = m_{B^0}/m_{D^{*\pm}}$. Perfect heavy quark symmetry, in the limit of infinite quark mass, implies equality between all form factors and ratios, $\mathcal{F}(w) = R_1(w) = R_2(w) = 1$. The finite masses of quarks can then be accounted for in corrections at zero hadronic recoil, resulting in $h_{A_1}(1) = \mathcal{F}(1) = 0.906$ [12]. Therefore, there are four independent parameters in this model used to calculate the expected yield of $B^0 \rightarrow D^{*-}\ell^+\nu_\ell$ events: $|V_{cb}|$, ρ^2 , $R_1(1)$ and $R_2(1)$. The values of these parameters are not calculated, but are instead extracted from fits to experimental data. We note that isolating the value of $|V_{cb}|$ from fits depends on knowing the scale factor $\mathcal{F}(1)$ to a high degree of certainty. As this number is subject to change, we present all results for $|V_{cb}|$ in the form $\mathcal{F}(1)\eta_{EW}|V_{cb}|$, except where cancellation occurs in ratios.

In the BGL parametrization, three power series

$$\begin{aligned} f(z) &= \frac{1}{P_{1+}(z)\phi_f(z)} \sum_{n=0}^{\infty} a_n^f z^n, \\ \mathcal{F}_1(z) &= \frac{1}{P_{1+}(z)\phi_{\mathcal{F}_1}(z)} \sum_{n=0}^{\infty} a_n^{\mathcal{F}_1} z^n, \\ g(z) &= \frac{1}{P_{1-}(z)\phi_g(z)} \sum_{n=0}^{\infty} a_n^g z^n, \end{aligned} \quad (8)$$

are related to the CLN form factors via

$$\begin{aligned} h_{A_1}(w) &= \frac{f(w)}{\sqrt{m_{B^0}m_{D^{*\pm}}}(1+w)}, \\ h_V(w) &= g(w)\sqrt{m_{B^0}m_{D^{*\pm}}}, \\ R_1(w) &= (w+1)m_{B^0}m_{D^{*\pm}} \frac{g(w)}{f(w)}, \\ R_2(w) &= \frac{w-r}{w-1} - \frac{\mathcal{F}_1(w)}{m_{B^0}(w-1)f(w)}. \end{aligned} \quad (9)$$

In these equations, the Blaschke factors, $P_{1\pm}$, are given by

$$P_{1\pm}(z) = \prod_{P=1}^n \frac{z - z_{\pm P}}{1 - z z_{\pm P}}, \quad (10)$$

where $z_{\pm P}$ is defined as

$$z_{\pm P} = \frac{\sqrt{t_+ - m_{\pm P}^2} - \sqrt{t_+ - t_-}}{\sqrt{t_+ - m_{\pm P}^2} + \sqrt{t_+ - t_-}}. \quad (11)$$

Here $t_{\pm} = (m_B \pm m_{D^*})^2$ and $m_{\pm P}$ denotes the P^{th} mass of the n $B_c^* 1^{\pm}$ resonances available (see Table I). The functions $\phi_i(z)$ are outer functions related to these Blaschke factors [5]. We have adopted the notation from Ref. [10], where $(n_f, n_g, n_{\mathcal{F}_1})$ refers to the highest power in each of these series that has not been fixed to zero. The Belle analysis used the BGL(1,0,2) configuration, with five free parameters, due to instability when more parameters were included. We will explore higher order expansions with the inclusion of additional LQCD constraints.

Unitarity constraints on the series coefficients require [4]

$$\sum_{n=0}^{\infty} (a_n^g)^2 < 1, \quad (12)$$

$$\sum_{n=0}^{\infty} [(a_n^f)^2 + (a_n^{\mathcal{F}_1})^2] < 1. \quad (12)$$

We note that by redefining these coefficients as $\tilde{a} = \eta_{\text{EW}} |V_{cb}| a$, we may extract a value for $|V_{cb}|$ using

$$\mathcal{F}(1) \eta_{\text{EW}} |V_{cb}| = \frac{1}{2m_{B^0} m_{D^{*\pm}}} \frac{|\tilde{a}_0^f|}{P_f(0) \phi_f(0)}. \quad (13)$$

A list of the inputs used in this analysis is given in Table I, with values chosen to remain consistent with [5]. We note that the value taken for $\mathcal{B}(D^0 \rightarrow K^- \pi^+)$ uses the fit result from the 2018 PDG [13]. There have been recent changes in this value, which impacts the normalization of measurements in this study and therefore directly affects the obtained values of $|V_{cb}|$. Updating $\mathcal{B}(D^0 \rightarrow K^- \pi^+)$ to the 2020 PDG fit value of $(3.950 \pm 0.031)\%$ [1], where a global fit over many charm modes is used, would reduce a measurement of $|V_{cb}|$ by approximately 0.75%, while the PDG average of direct measurements, $(3.909 \pm 0.034)\%$, would change the value by approximately 0.2%.

III. THE CHOLESKY DECOMPOSITION METHOD

A common method of measuring free parameters is via a χ^2 fit, maximizing the likelihood of observing an obtained binned data set. This is achieved by an algorithm that iterates through different values of a set of parameters, \mathbf{x} , to minimize a χ^2 variable, defined typically as

$$\chi^2 = \sum_{i,j} (N_i^{\text{obs}} - N_i^{\text{exp}}) \mathcal{C}_{ij}^{-1} (N_j^{\text{obs}} - N_j^{\text{exp}}), \quad (14)$$

where N_i^{obs} is the number of events observed in bin i of the data sample, N_i^{exp} is the number of events expected in bin i , determined from theory using \mathbf{x} , and \mathcal{C}^{-1} is the inverse of the covariance matrix. The correlations between observed values are related to the covariance matrix by

$$\rho(i, j) = \frac{\mathcal{C}_{ij}}{\sigma_i \sigma_j}, \quad (15)$$

TABLE I. The full set of inputs used in this study. Both the CLN and the BGL fits use the common input, in addition to the data yields and detector responses published in Ref. [5]. The uncertainties listed are incorporated into the global systematic covariance matrix.

Common Input	
η_{EW}	1.0066
$h_{A_1}(1) = \mathcal{F}(1)$	0.906
m_{B^0}	$5.27963 \pm 0.15 \text{ GeV}/c^2$
$m_{D^{*\pm}}$	$2.01026 \pm 0.05 \text{ GeV}/c^2$
τ_{B^0}	$(1.520 \pm 0.004) \times 10^{-12} \text{ s}$
$\mathcal{B}(D^{*+} \rightarrow D^0 \pi^+)$	0.6770 ± 0.005
$\mathcal{B}(D^0 \rightarrow K^- \pi^+)$	0.0389 ± 0.0004
G_F	$1.16637 \times 10^{-5} \text{ GeV}^{-2} (\hbar c)^3$
$n_{B\bar{B}}$ (Belle)	$(772 \pm 11) \times 10^6$
BGL Input	
$B_c^* 1^+$ masses	6.730 GeV/c^2
	6.736 GeV/c^2
	7.135 GeV/c^2
	7.142 GeV/c^2
	7.280 GeV/c^2
$B_c^* 1^-$ masses	6.337 GeV/c^2
	6.899 GeV/c^2
	7.012 GeV/c^2
	7.280 GeV/c^2
	7.280 GeV/c^2
n_I	2.6
$\chi^T(+u)$	$5.28 \times 10^{-4} (\text{GeV}/c^2)^{-2}$
$\chi^T(-u)$	$3.07 \times 10^{-4} (\text{GeV}/c^2)^{-2}$

where σ_i is the standard deviation of the i^{th} measurement (*i.e.* $\sigma_i^2 = \text{var}(i) = \mathcal{C}_{ii}$).

In evaluating χ^2 , the diagonal elements ($i = j$) must add a positive value, while those off the diagonal may add a negative value. Data samples with large off-diagonal correlations can therefore have a lower χ^2 than an identical data sample with correlations closer to zero. This can place a minimum χ^2 at parameter values away from those which provide the nominal fit (*i.e.* the expected events from the fit will appear biased away from the observed data). In particular, bias can be introduced because of large systematic uncertainties in normalization factors, known as the D'Agostini effect [14]. Due to this effect, it becomes difficult to determine the true value and total uncertainty of a parameter.

To determine the uncertainty of a parameter in cases where correlations are high we use a toy Monte Carlo (MC) method incorporating the Cholesky decomposition [15] to avoid directly including systematic uncertainties from normalization factors. A positive-definite covariance matrix, \mathcal{C} , undergoes a Cholesky decomposition such that

$$\mathcal{C} = LL^T, \quad (16)$$

where L is a lower triangular matrix. A vector u is cre-

ated where each element is a random number taken from a Gaussian distribution with a mean of 0 and variance 1. The vector for the observed data is then fluctuated by

$$N'_{obs} = N_{obs} + Lu, \quad (17)$$

where Lu maintains the desired covariance properties [16]. The data is fluctuated many times according to its uncertainty profile, and the fit procedure repeated to find a distribution of parameter values. This process represents the randomness in measurements of the data that are affected by systematic or statistical uncertainties and correlations incorporated in the covariance matrix. A Gaussian function can then be fit to these parameter distributions and the mean and width can be taken to be the nominal value and uncertainty of each parameter, respectively. Assuming that all fits converged without reaching boundary conditions, the mean obtained from the fit without the toy MC method will be equal to the mean obtained from the Gaussian fit. Likewise, the standard deviation calculated from the distribution of results will be equal to the width obtained from the Gaussian fit and it is through this latter method that central values and uncertainties are calculated in this analysis. In the appendix, we discuss the consequences of high systematic correlations in the Belle analysis, owing to dominant scale uncertainties, and verify that the toy MC method with Cholesky decomposition does not bias the fit results.

A. Using the Cholesky decomposition method

In the Belle paper [5], the free parameters in both the BGL and CLN parametrization for $B^0 \rightarrow D^{*-}\ell^+\nu_\ell$ decays were measured. The systematic uncertainties were determined through a toy MC approach and were published as a systematic uncertainty correlation matrix. Although the statistical correlations between the bins of the different observables were small, the systematic correlations were close to 1 almost everywhere. A fit using the data provided obtains the same central values only when the statistical covariance matrix is used in the χ^2 function. However, if systematic uncertainty is introduced into the covariance matrix in a “naive” way, where

$$\mathcal{C}_{\text{total}} = \mathcal{C}_{\text{stat.}} + \mathcal{C}_{\text{sys.}}, \quad (18)$$

the minimizing algorithm returns a lower χ^2 value but with a clear bias in the expected yield and fit parameters. These results are discussed in Appendix A.

In order to obtain results based on the available data, a toy MC sample was produced using the statistical and systematic covariance matrices separately via the Cholesky decomposition method. The minimizing algorithm was applied to measure the parameter values for 10^4 iterations. We note that the systematic uncertainties that are multiplied into the correlation matrix to obtain the covariance matrix were calculated using the theoretical yield, not the observed yield to avoid bias from the

D’Agostini effect [17]. This approach is consistent with the Belle paper.

The fit parameter distributions have a Gaussian shape, where the central value of each parameter is taken from the nominal fit without the toy MC method and the statistical and systematic uncertainties are taken from the widths of the Gaussian distributions from their respective toy MC samples. The mean values for the parameters agree across the three measurements. We observe in Fig. 1 that the yields obtained from the CLN and BGL(1,0,2) parametrizations are in excellent agreement, and model the data well. The results for CLN and BGL(1,0,2) are given in the first columns of Tables III and IV, respectively. The systematic uncertainties are largest in $\mathcal{F}(1)\eta_{EW}|V_{cb}|$, as it is associated to overall normalization, but the central values are consistent between CLN and BGL(1,0,2) within statistical uncertainty alone. The reported $B^0 \rightarrow D^{*-}\ell^+\nu_\ell$ branching fractions are found to be in agreement with the expected PDG value [13], indicating minimal bias has been introduced in the fit, as was expected from using the toy MC method with the Cholesky decomposition.

These results are consistent with the Belle analysis, noting that the overall sign of the BGL coefficients is arbitrary. The systematic uncertainties reported here differ to results presented in [5]. This is attributable to using a forward-folding method where fits were applied to background-subtracted data and all correlations between uncertainties were taken to be linear. This may not consistently represent the exact nature of the correlations present in the data, which could have been non-linear in some cases but were taken into account in the original study.

IV. COMPARING RESULTS WITH ELECTRONS AND MUONS IN THE FINAL STATE

The results published by the Belle analysis provided yields and uncertainties for $B^0 \rightarrow D^{*-}\ell^+\nu_\ell$ for $\ell = e, \mu$. Each mode can be analyzed separately as a test of lepton flavor universality and to check for consistency in the fits, as seen in Table IV and Table VI of [5]. It was seen that all fit coefficients were consistent with one another, with the exception of $R_1(1)$ in CLN and \tilde{a}_0^g in BGL(1,0,2), where we note that $R_1(1)$ is directly proportional to \tilde{a}_0^g in BGL from Eq. 9. We repeat this analysis using the Cholesky decomposition method and observe the same features as the previous measurement. As a further test of lepton flavor universality, we measure the ratio of the fit parameters for CLN and BGL(1,0,2), cancelling off all systematic uncertainties except for lepton identification. The results are listed in Table II. All ratios in the CLN parametrization remain consistent with unity, except for $R_1(1)$. For BGL, large statistical uncertainties reduce the significance of the results for higher order coefficients. However, all coefficients, and $|V_{cb}|$ in particular, are con-

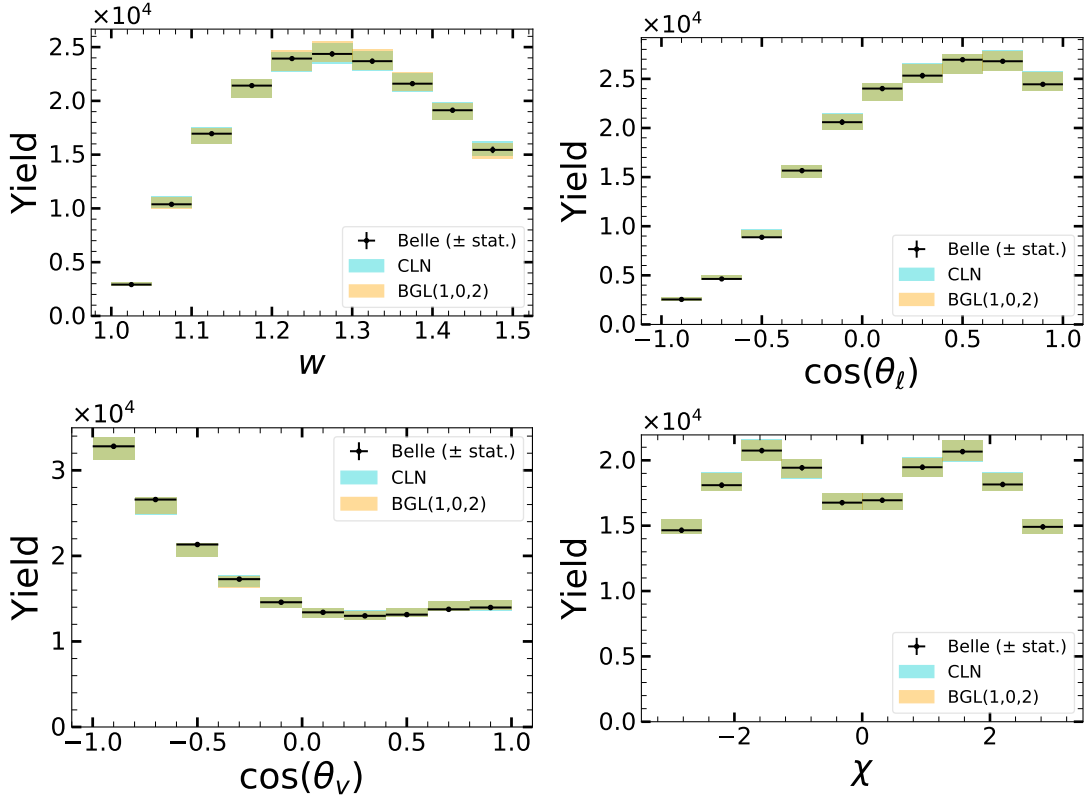


FIG. 1. The measured binned yields (data points) with statistical uncertainty for each observable of the $B^0 \rightarrow D^{*-} \ell^+ \nu_\ell$ decay overlaid with both the CLN (cyan) and BGL(1,0,2) (orange) parametrization fit results. The statistical and systematic uncertainties in the fits are determined via the toy MC method with the Cholesky decomposition and added in quadrature for these graphs. As the analysis uses a forward-folding approach, the yields predicted by the fit results are also binned. The results from the CLN and BGL parametrizations are in agreement with each other and with the data.

sistent between the electron and muon final states, apart from \tilde{a}_0^g . We note that this tension is present when using different configurations of CLN and BGL and after introducing additional constraints from LQCD calculations of form factors as non-zero recoil. While the consistency in the overall rate demonstrates lepton flavor universality, we note that the observed difference in $R_1(1)$ or \tilde{a}_0^g could be due to some minor experimental effects related to lepton flavor specific acceptance or background from mis-identified hadrons. From here on we consider only the combined sample and focus on the determination of $|V_{cb}|$.

V. HIGHER ORDER CLN

The form factor ratios for $B^0 \rightarrow D^{*-} \ell^+ \nu_\ell$ are defined as ratios of the vector and axial-vector form factors:

$$\begin{aligned} R_1(w) &= \frac{h_V(w)}{h_{A_1}(w)}, \\ R_2(w) &= \frac{h_{A_3}(w) + r_{D^*} h_{A_2}(w)}{h_{A_1}(w)}. \end{aligned} \quad (19)$$

In the heavy quark limit, $h_{A_1} = h_{A_3} = h_V = \xi$ and $h_{A_2} = 0$, where ξ is the Isgur-Wise function [18, 19] and $r_{D^*} = m_{D^{*\pm}}/m_{B^0}$. These form factors can be expanded in powers of $\Lambda_{\text{QCD}}/m_{c,b}$ and α_s . It is convenient to parametrize deviations from the heavy quark limit using Eq. 19 which satisfy $R_{1,2}(w) = 1 + \mathcal{O}(\Lambda_{\text{QCD}}/m_{c,b}, \alpha_s)$ in the $m_{c,b} \gg \Lambda_{\text{QCD}}$ limit.

We introduce the parametrization discussed in Ref. [20], “CLNnoR”, in which

$$\begin{aligned} R_1(w) &= R_1(1) + (w-1)R'_1(1), \\ R_2(w) &= R_2(1) + (w-1)R'_2(1), \end{aligned} \quad (20)$$

and fit $R'_1(1)$ and $R'_2(1)$ as additional floating parameters. CLNnoR is a simple modification of the CLN parametrization that removes QCD sum rule inputs and the condition $R_{1,2}(w) = 1 + \mathcal{O}(\Lambda_{\text{QCD}}/m_{c,b}, \alpha_s)$ but still relies on heavy quark symmetry and model-dependent input on subleading Isgur-Wise functions due to constraints on the cubic polynomial used to describe the form factor h_{A_1} . These heavy quark symmetry constraints can be further loosened to form the model “CLNnoHQS”, in which h_{A_1} from Eq. 9 is parametrized by a quadratic polynomial in z , with unconstrained coefficients:

$$h_{A_1}(w) = h_{A_1}(1)[1 - 8\rho^2 z + (53c_{D^*} - 15)z^2], \quad (21)$$

TABLE II. Ratios of fitted parameters in electron and muon modes in the CLN and BGL(1,0,2) parametrizations. The systematic uncertainties listed are only those from lepton identification, as all others cancel in the ratios. Note that from Eq. 13, the ratios for \tilde{a}_0^f and $|V_{cb}|$ are equal in BGL and therefore only $|V_{cb}|$ is listed.

CLN e/μ ratio	val. \pm stat. \pm sys.	BGL(1,0,2) e/μ ratio	val. \pm stat. \pm sys.
ρ^2	$0.97 \pm 0.07 \pm 0.02$	\tilde{a}_1^f	$1.5 \pm 1.1 \pm 0.2$
$R_1(1)$	$0.84 \pm 0.05 \pm 0.02$	$\tilde{a}_1^{\mathcal{F}_1}$	$1.2 \pm 0.7 \pm 0.05$
$R_2(1)$	$1.01 \pm 0.06 \pm 0.01$	$\tilde{a}_2^{\mathcal{F}_1}$	$1.2 \pm 1.1 \pm 0.04$
$ V_{cb} $	$1.01 \pm 0.01 \pm 0.01$	\tilde{a}_0^g	$0.85 \pm 0.04 \pm 0.01$
		$ V_{cb} $	$1.00 \pm 0.02 \pm 0.01$

where setting $c_{D^*} = \rho^2$ will return the original CLN parametrization truncated to its second order.

We performed fits to the $B^0 \rightarrow D^{*-} \ell^+ \nu_\ell$ data for the three different CLN models and the results are summarized in Table III. Large uncertainties are seen in the results for CLNnoR and CLNnoHQS. The contours for the standard CLN and BGL(1,0,2) models are shown in Fig. 2, where smooth curves indicate that the true minimum in the log-likelihood function was found and therefore the variation in parameters with respect to each other around this minimum can be determined.

Figure 3 shows the form factor ratios R_1 and R_2 , the form factor h_{A_1} divided by its value at $w = 1$, and $\mathcal{F}(1)\eta_{EW}|V_{cb}|$ for the three CLN fit configurations as a function of the hadronic recoil, w . The combination of the statistical and systematic uncertainties in the fits are shown for each configuration, obtained from the toy MC method with the Cholesky decomposition. We note that in both CLN and BGL, the uncertainty in the plots of $h_{A_1}(w)$ reduces to zero at $w = 1$, and has been presented as a ratio to avoid assuming the value and uncertainty of $h_{A_1}(1)$. From Eq. 9 in CLN, and because $\eta_{EW}|V_{cb}|$ has been absorbed into the BGL coefficients, the form factor will converge to the fixed value of $h_{A_1}(1) = 0.906$. A further toy MC analysis could be applied to the fit results to estimate the effect of the uncertainty in $h_{A_1}(1)$ for values at higher hadronic recoil, but it would have no effect on the overall convergence of the fits and is therefore beyond the scope of this analysis.

The distribution of $\mathcal{F}(1)\eta_{EW}|V_{cb}|$ shows that the CLNnoR and CLNnoHQS parametrizations have large uncertainty at low hadronic recoil, with their central values diverging from the standard CLN value, but remaining compatible within uncertainty. At larger values of hadronic recoil, this form factor becomes less sensitive to the fit parameters. The results of CLNnoR and CLNnoHQS for the form factor ratios $R_1(w)$ and $R_2(w)$ show large uncertainties near zero and maximal recoil, remaining consistent with CLN. The compatibility between these two configurations and the more model-dependent CLN are an indication that the heavy quark symmetry assumed in the structure of CLN remains present when these assumptions are no longer included. This is in contrast to the study performed in Ref. [20] using the tagged Belle data set [6] where the fits were also seen to return

a reasonable χ^2 but may not have fully incorporated systematic uncertainties leading to smaller error bands and bias from normalization uncertainties. Our results are found to be more similar to those from a study using BGL [10], where the plots of form factor ratios are consistent with expected theoretical results for heavy quark symmetry.

VI. HIGHER ORDER BGL

The form factors, f , g and \mathcal{F}_1 in the BGL parametrization are defined as a power series of $z(w)$. We can perform fits to the data for truncations at varying order, including the systematic uncertainties as described in Section II and the constraints given in Eq. 12. The results of the BGL fit with expansions (1, 0, 2) and (1, 1, 2) are given in Table IV, where fits to expansions with more free parameters do not converge with the given data set. From Table IV, we note that increasing the power in the z expansions also has a considerable impact on the results, including shifting the value obtained for $|V_{cb}|$ lower by 3% but remaining compatible within systematic uncertainties. This shift can also be seen in Fig. 4, where adding parameters to the fit has caused large deviations and uncertainties in form factor plots, similar to the effects seen in CLNnoR and CLNnoHQS. These shapes are consistent with the results seen in [10] where uncertainties dominate the hadronic recoil end points. Form factors obtained by LQCD calculations [21] appear to have a shape more consistent with those from the BGL(1,0,2) and CLN configurations. From this, we conclude that adding further free parameters into the fits to this data set without further constraints introduces instability in both parametrization models and although most results remain consistent within large uncertainties, useful results become difficult to extract.

VII. ADDITIONAL DATA FROM LQCD

The use of data from LQCD calculations of form factors at non-zero recoil is an important recent development in the measurement of $|V_{cb}|$ [22]. By providing

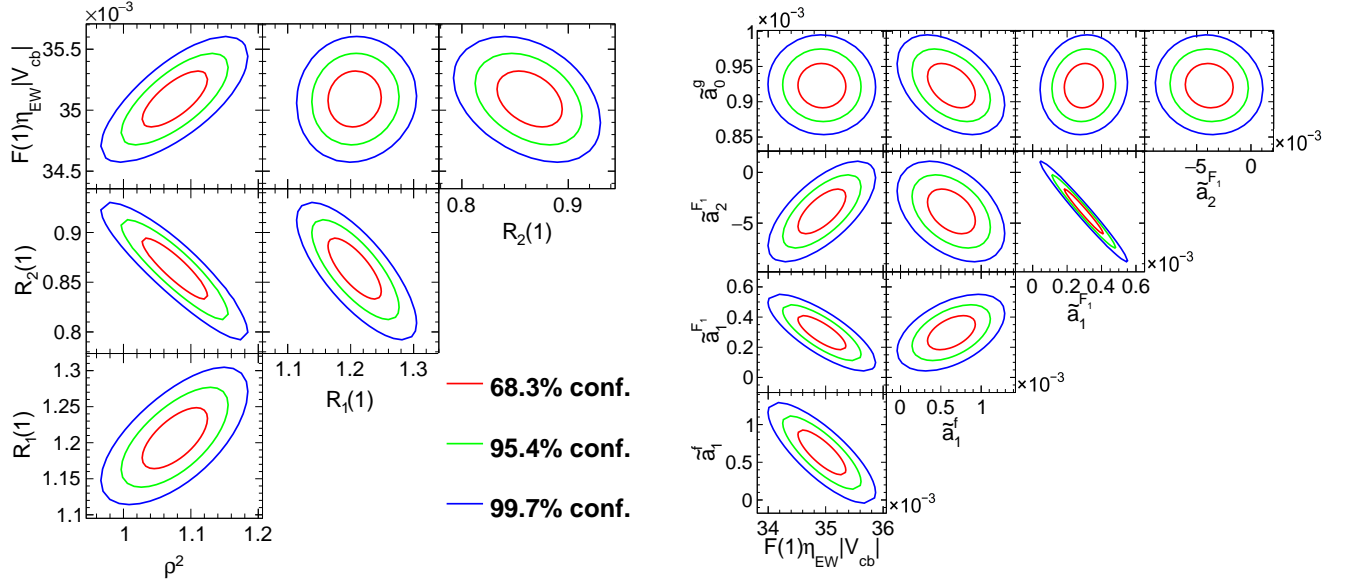


FIG. 2. 2-D contours of pairs of fit parameters for CLN (left) and BGL(1,0,2) (right) at 68.3%, 95.4% and 99.7% confidence levels. Note that from Eq. 13, the correlations for \tilde{a}_0^f and $\mathcal{F}(1)\eta_{EW}|V_{cb}|$ are equal in BGL and therefore only the latter is shown.

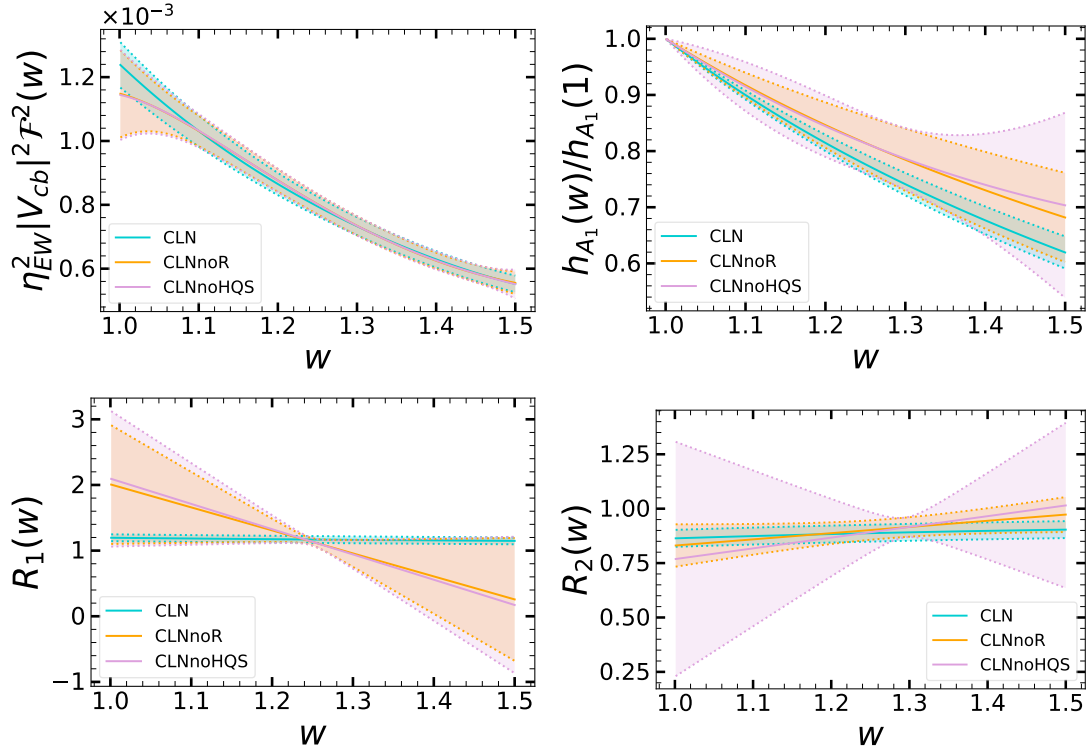


FIG. 3. $\eta_{EW}^2|V_{cb}|^2\mathcal{F}^2$, $h_{A_1}(w)/h_{A_1}(1)$, R_1 and R_2 as a function of the hadronic recoil, w , for the CLN, CLNnoR and CLNnoHQS scenarios. The uncertainty bands correspond to the sum of the statistical and systematic uncertainties. The solid lines correspond to the central values from the fit with no toy MC and the uncertainty bands correspond to the combination of the statistical and systematic uncertainties obtained from the standard deviation of the distribution of the function values at each point in w .

TABLE III. Fitted parameters in the CLN, CLNnoR and CLNnoHQS scenarios for the combined dataset (electron and muon modes). The uncertainties listed are statistical and systematic, respectively. The branching ratio and χ^2 value are obtained from the fit. No additional input from LQCD has been used.

Parameter	CLN	CLNnoR	CLNnoHQS
ρ^2	$1.09 \pm 0.04 \pm 0.05$	$0.89 \pm 0.10 \pm 0.15$	$0.93 \pm 0.33 \pm 0.31$
$R_1(1)$	$1.20 \pm 0.03 \pm 0.02$	$2.01 \pm 0.43 \pm 0.48$	$2.10 \pm 0.56 \pm 0.48$
$R_2(1)$	$0.86 \pm 0.02 \pm 0.02$	$0.83 \pm 0.06 \pm 0.04$	$0.77 \pm 0.32 \pm 0.22$
$R'_1(1)$	-0.12	$-3.5 \pm 1.8 \pm 1.9$	$-3.9 \pm 2.2 \pm 1.9$
$R'_2(1)$	0.11	$0.29 \pm 0.15 \pm 0.16$	$0.49 \pm 1.09 \pm 0.74$
c_{D^*}	ρ^2	ρ^2	$1.0 \pm 1.4 \pm 1.0$
$\mathcal{F}(1)\eta_{EW} V_{cb} \times 10^3$	$35.2 \pm 0.2 \pm 0.8$	$33.9 \pm 0.7 \pm 1.4$	$33.8 \pm 0.7 \pm 1.4$
$\mathcal{B}(B^0 \rightarrow D^{*-} \ell^+ \nu_\ell)$	4.93%	4.92%	4.92%
χ^2/ndf	40.8/36	34.7/34	34.7/33

TABLE IV. Fitted parameter values in BGL(1,0,2) and BGL(1,1,2) for the combined dataset (electron and muon modes). The uncertainties listed are statistical and systematic, respectively. The branching ratio and χ^2 value are obtained from the fit, and $\mathcal{F}(1)\eta_{EW}|V_{cb}|$ is calculated from Eq. 13. Configurations with higher order coefficients do not converge without additional input from LQCD.

Parameter $\times 10^3$	BGL(1,0,2)	BGL(1,1,2)
\tilde{a}_0^f	$0.506 \pm 0.004 \pm 0.014$	$0.490 \pm 0.008 \pm 0.018$
\tilde{a}_1^f	$0.63 \pm 0.20 \pm 0.36$	$1.36 \pm 0.34 \pm 0.57$
\tilde{a}_2^f	0.0	0.0
\tilde{a}_0^g	$0.92 \pm 0.02 \pm 0.01$	$1.55 \pm 0.25 \pm 0.28$
\tilde{a}_1^g	0.0	$-22.3 \pm 9.1 \pm 9.8$
\tilde{a}_2^g	0.0	0.0
$\tilde{a}_1^{\mathcal{F}_1}$	$0.30 \pm 0.08 \pm 0.10$	$0.37 \pm 0.09 \pm 0.12$
$\tilde{a}_2^{\mathcal{F}_1}$	$-3.8 \pm 1.5 \pm 1.4$	$-3.7 \pm 1.5 \pm 1.5$
$\mathcal{F}(1)\eta_{EW} V_{cb} $	$34.9 \pm 0.3 \pm 1.0$	$33.8 \pm 0.5 \pm 1.3$
$\mathcal{B}(B^0 \rightarrow D^{*-} \ell^+ \nu_\ell)$	4.92%	4.92%
χ^2/ndf	38.5/35	34.8/34

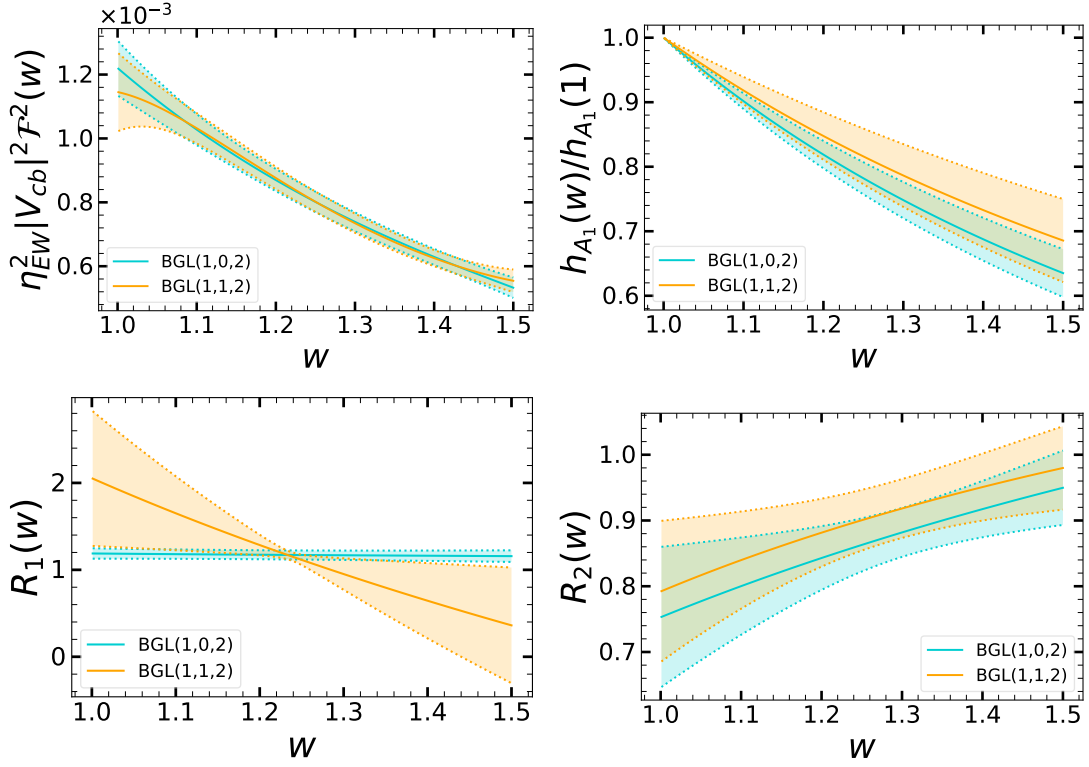


FIG. 4. The form factors and ratios $\eta_{EW}^2 |V_{cb}|^2 \mathcal{F}^2$, $h_{A_1}(w)/h_{A_1}(1)$, R_1 and R_2 as a function of the hadronic recoil, w , for BGL(1,0,2) and BGL(1,1,2). The central values and uncertainties are calculated via the same method as Fig. 3.

precise input near zero recoil, form factors can be much better constrained than from experimental information alone, owing to the presence of a low-momentum (slow) pion affecting efficiencies in this region of phase space. Results have been presented in Ref. [23] (Fermilab/MILC collaboration), which has a blinded normalization factor, and Ref. [21] (JLQCD collaboration), which presents preliminary unblinded results.

This paper examines the impact of LQCD inputs on constraining higher order parametrizations, leading to a reduction in model dependence in the evaluation of $|V_{cb}|$. Although $\mathcal{F}(1)\eta_{EW}|V_{cb}|$ values are quoted, the results are based on preliminary inputs that are subject to change. While other studies have used form factors evaluated at non-zero recoil in discussions on implications for $R(D^*)$ [24] or have included additional form factor constraints from light cone sum rules [25], this analysis features a novel approach for including data from LQCD as additional constraints for determining $B^0 \rightarrow D^{*-}\ell^+\nu_\ell$ form factors in various parametrization scenarios. Four points related to h_V and h_{A_1} at different values of hadronic recoil were used:

$$\begin{aligned} h_{A_1}(1.04)/h_{A_1}(1) &= 0.9534 \cdot (1 \pm 1.3\% \pm 3.4\%), \\ h_{A_1}(1.08)/h_{A_1}(1) &= 0.9093 \cdot (1 \pm 1.3\% \pm 3.5\%), \\ h_V(1.04)/h_V(1) &= 0.9403 \cdot (1 \pm 2.4\% \pm 6.8\%), \\ h_V(1.08)/h_V(1) &= 0.9040 \cdot (1 \pm 2.4\% \pm 6.9\%), \end{aligned} \quad (22)$$

with $h_{A_1}(1) = 0.906$ and $h_V(1) = 1.18$ [21]. While the uncertainties provided were asymmetric, we have simplified their inclusion by conservatively taking the maximum value of the upper and lower errors when symmetrizing. These points were added to the N_{obs} vector from Eq. 14, expanding it to size $40 + 4$, while the correlations between these values (obtained from preliminary estimates via private correspondence with the JLQCD group and listed in Table VII) were appended to the original statistical covariance matrix in a block-diagonal manner. The N_{exp} vector was expanded to include the calculated values for the corresponding form factors given a set of values for the free parameters. The χ^2 minimization approach was applied with the Cholesky toy MC method to obtain results for various BGL and CLN parametrizations.

A. Impact of LQCD constraints on fits

We apply the toy MC method using Cholesky decomposition to obtain measurements of the free parameters in all the CLN and BGL configurations listed previously. As the exact LQCD values used are not published, the focus of this analysis is to explore the effects of additional constraints rather than perform a new measurement for $|V_{cb}|$ and the sensitivity to these values is explored in the following subsection. As such, the values presented

in Tables V and VI should only be compared with each other.

Most fit parameters are reasonably consistent between the different configurations, while the values of $\mathcal{F}(1)\eta_{EW}|V_{cb}|$ are in agreement in all scenarios. The inclusion of LQCD constraints has not been found to introduce a bias in the normalization of the fits as the measured $\mathcal{B}(B^0 \rightarrow D^{*-}\ell^+\nu_\ell)$ values are consistent with previous measurements, and the yields, as seen in Fig. 5, are compatible with the data. Overall we find that all fit scenarios model the data well, where the CLN configuration has a p-value of 0.37 and all other scenarios have similar values. We find that in the BGL(2,2,2) scenario the value for \tilde{a}_2^g will often reach the boundary condition set by Eq. 12 and so its uncertainties cannot be considered Gaussian-shaped. Instead, they are calculated in an asymmetric manner where the mean of the difference between each value of \tilde{a}_2^g and its lower bound is taken as the lower uncertainty and the upper uncertainty is taken as the standard deviation minus this number. This indicates that the BGL(2,2,2) fit is not as reliable as those of lower order. However, the measurement and uncertainty of $\mathcal{F}(1)\eta_{EW}|V_{cb}|$ remains relatively unaffected.

A smaller uncertainty is seen for higher order expansions in BGL with LQCD input, compared to fits without. Figure 6 emphasizes this, where fits using the BGL parametrization with constraints from LQCD are compatible with the additional h_V data points at non-zero recoil. As discussed in Ref. [11] the BGL(1,0,2) configuration can be considered over-constrained with limited flexibility and therefore not the optimal fit configuration in BGL. Using LQCD constraints, we find little difference between BGL configurations for the CLN-equivalent form factors and form factor ratios at low hadronic recoil, while at larger values, the order of the power series for the three BGL form factors causes a divergence in R_1 . This is depicted in Figs. 7 and 8, which show a significant reduction in uncertainties when compared to Figs. 3-4. Similar behavior is seen in the CLNnoR and CLNnoHQs scenarios in R_1 .

These results suggest that obtaining a model-independent value of $|V_{cb}|$ is possible with the use of additional constraints, as effects from having a large parameter space are reduced.

B. Sensitivity to LQCD inputs

We explore the sensitivity of $\mathcal{F}(1)\eta_{EW}|V_{cb}|$ to these values to determine whether the final result will change significantly if constraints and correlations were to change. Two values were taken at $w = 1.04, 1.08$ for each of $h_{A_1}(w)$ and $h_V(w)$, as this was the minimum amount of extra information required for the BGL(2,2,2) parametrization to converge. To measure what effect these values have on the fit results, we establish a toy MC analysis using the standard CLN parametrization. When fixed, the four non-zero recoil values for this toy

MC study are set to

$$\begin{aligned} h_{A_1}(1.04)/h_{A_1}(1) &= (0.95 \pm 0.05), \\ h_{A_1}(1.08)/h_{A_1}(1) &= (0.91 \pm 0.05), \\ h_V(1.04)/h_V(1) &= (0.95 \pm 0.05), \\ h_V(1.08)/h_V(1) &= (0.90 \pm 0.05). \end{aligned} \quad (23)$$

The correlations between these are given in Table VII.

These values have been rounded off from those originally used, with simplified uncertainties. Each correlation was unfixed individually and set to 100 different values spanning 0 to 1 while the others remained fixed and then the fitting algorithm was applied. The non-zero recoil values were treated in two different ways, where each of the four values were varied separately or the two values associated with a given function were varied together. The ratio of the form factors h_{A_1} and h_V between their value at $w = 1.04$ and $w = 1$ were varied between 0.9 – 1.0 and those at $w = 1.08$ were varied between 0.85 – 0.95, covering a range of different possible slopes. In both treatments of the non-zero recoil values, the range of values obtained for $|V_{cb}|$ changed by at most 0.1% while the largest change over any other fit parameter was 2%, which is smaller than the systematic uncertainty calculated in the main analysis. The fit parameters as a function of each correlation were also found to vary by at most 1%, except around finely tuned points during which the correlation matrix has eigenvalues nearing zero, at which point the entries in \mathcal{C}^{-1} diverge to infinity. From this we conclude that any results for $|V_{cb}|$ are not highly sensitive to the actual values of the additional form factor constraints at non-zero recoil, under the assumption that the correlation matrix remains invertible.

VIII. CONCLUSION

We have performed a study of fits to exclusive $B^0 \rightarrow D^{*-}\ell^+\nu_\ell$ measurements for the determination of $|V_{cb}|$, based on the Belle 2019 untagged measurement. We used preliminary results from the JLQCD group for form factor calculations at non-zero hadronic recoil as additional constraints and find that fits with higher-order parametrizations will reliably converge.

The $\mathcal{F}(1)\eta_{EW}|V_{cb}|$ results obtained from each of the different methods described in this paper are shown in Fig. 9.

We have used a toy MC approach making use of the covariance properties of the Cholesky decomposition to take into account scale-error dominant systematic uncertainties in order to avoid bias. We obtain form factor parameters in BGL(1,0,2) and CLN consistent with the Belle 2019 measurement. The values measured for $\mathcal{F}(1)\eta_{EW}|V_{cb}|$ are $(35.2 \pm 0.2 \pm 0.8) \times 10^{-3}$ and $(34.9 \pm 0.3 \pm 1.0) \times 10^{-3}$ for CLN and BGL(1,0,2), respectively, with statistical and systematic uncertainties. We take the ratio of results in the electron final state with

TABLE V. Fitted parameters in the CLN, CLNnoR and CLNnoHQS scenarios based on the combined electron and muon dataset as well as form factors from JLQCD calculated at non-zero recoil. The uncertainties listed are statistical and systematic, respectively. The branching ratio is obtained from the fit.

Parameter	CLN	CLNnoR	CLNnoHQS
ρ^2	$1.10 \pm 0.03 \pm 0.06$	$1.05 \pm 0.04 \pm 0.07$	$0.80 \pm 0.18 \pm 0.24$
$R_1(1)$	$1.21 \pm 0.03 \pm 0.02$	$1.29 \pm 0.02 \pm 0.02$	$1.25 \pm 0.02 \pm 0.02$
$R_2(1)$	$0.86 \pm 0.02 \pm 0.02$	$0.80 \pm 0.06 \pm 0.04$	$0.99 \pm 0.17 \pm 0.16$
$R'_1(1)$	-0.12	$-0.45 \pm 0.10 \pm 0.06$	$-0.26 \pm 0.10 \pm 0.11$
$R'_2(1)$	0.11	$0.26 \pm 0.14 \pm 0.14$	$-0.39 \pm 0.57 \pm 0.55$
c_{D^*}	ρ^2	ρ^2	$-0.06 \pm 0.71 \pm 0.80$
$\mathcal{F}(1)\eta_{EW} V_{cb} \times 10^3$	$35.2 \pm 0.2 \pm 0.8$	$34.9 \pm 0.2 \pm 0.9$	$34.6 \pm 0.3 \pm 1.0$
$\mathcal{B}(B^0 \rightarrow D^{*-} \ell^+ \nu_\ell)$	4.93%	4.92%	4.92%
χ^2/ndf	42.3/40	38.8/38	37.5/37

TABLE VI. Fitted parameters in BGL(1,0,2), BGL(1,1,2) and BGL(2,2,2) for combined electron and muon modes using data from LQCD calculations of form factors at non-zero recoil as additional constraints. The uncertainties listed are statistical and systematic, respectively. We note that in BGL(2,2,2) \tilde{a}_2^g is seen to reach the end point in the constraint imposed by Eq. 12 and has listed with asymmetric uncertainties.

The branching ratio is obtained from the fit and $\mathcal{F}(1)\eta_{EW}|V_{cb}|$ is calculated from Eq. 13.

Parameter $\times 10^3$	BGL(1,0,2)	BGL(1,1,2)	BGL(2,2,2)
\tilde{a}_0^f	$0.506 \pm 0.003 \pm 0.013$	$0.505 \pm 0.004 \pm 0.013$	$0.501 \pm 0.003 \pm 0.013$
\tilde{a}_1^f	$0.61 \pm 0.18 \pm 0.31$	$0.66 \pm 0.17 \pm 0.31$	$1.41 \pm 0.55 \pm 0.85$
\tilde{a}_2^f	0.0	0.0	$-19.6 \pm 15.8 \pm 20.2$
\tilde{a}_0^g	$0.93 \pm 0.02 \pm 0.01$	$1.00 \pm 0.02 \pm 0.02$	$0.96 \pm 0.02 \pm 0.04$
\tilde{a}_1^g	0.0	$-2.33 \pm 0.60 \pm 0.70$	$0.01 \pm 0.92 \pm 1.50$
\tilde{a}_2^g	0.0	0.0	$-38.2^{+3.1}_{-0.3} {}^{+10.3}_{-2.3}$
$\tilde{a}_1^{\mathcal{F}_1}$	$0.30 \pm 0.06 \pm 0.08$	$0.29 \pm 0.06 \pm 0.08$	$0.29 \pm 0.07 \pm 0.09$
$\tilde{a}_2^{\mathcal{F}_1}$	$-4.0 \pm 1.1 \pm 1.1$	$-3.6 \pm 1.2 \pm 1.2$	$-3.0 \pm 1.5 \pm 1.4$
$\mathcal{F}(1)\eta_{EW} V_{cb} $	$34.9 \pm 0.2 \pm 0.9$	$34.9 \pm 0.2 \pm 0.9$	$34.6 \pm 0.2 \pm 0.9$
$\mathcal{B}(B^0 \rightarrow D^{*-} \ell^+ \nu_\ell)$	4.92%	4.92%	4.92%
χ^2/ndf	40.2/39	38.9/38	37.6/36

those of the muon, including only uncertainty correlations related to lepton identification, and measure values consistent with lepton flavor universality for $|V_{cb}|$ at $1.01 \pm 0.01 \pm 0.01$ for CLN and $1.00 \pm 0.02 \pm 0.01$ for BGL(1,0,2). We find a tension between electrons and muons in fit parameters associated with the form factor ratio $R_1(w)$ in both methods.

We perform fits to the CLN parametrization without the requirement of heavy quark symmetry on one or both of the form factor ratios and h_{A_1} , finding compatible results for the form factors and $\mathcal{F}(1)\eta_{EW}|V_{cb}|$. This demonstrates that the heavy quark symmetry assumptions used in the modelling of CLN are valid and that the results are not indicative of any breakdown in heavy quark symmetry or the use of subleading Isgur-Wise functions.

With the inclusion of JLQCD non-zero recoil constraints we achieve a model-independent result for $\mathcal{F}(1)\eta_{EW}|V_{cb}|$, $(34.9 \pm 0.2 \pm 0.9) \times 10^{-3}$ in BGL(1,1,2). The fit at this order was found to be stable, whereas

higher orders often approached unitarity bounds. Assuming a value of $\mathcal{F}(1)$ from Eq. 2 we find $|V_{cb}| = (38.0 \pm 0.3 \pm 1.0) \times 10^{-3}$, which remains to be in tension with the inclusive determination.

ACKNOWLEDGEMENTS

We would like to thank T. Kaneko from KEK, Tsukuba, E. Kou from IJCLab, Orsay, and the JLQCD collaboration for their important contributions to lattice calculations and guidance in this analysis. We also thank the Japan Society for the Promotion of Science (JSPS) and the Australian Research Council (ARC DP190101991) for their support.

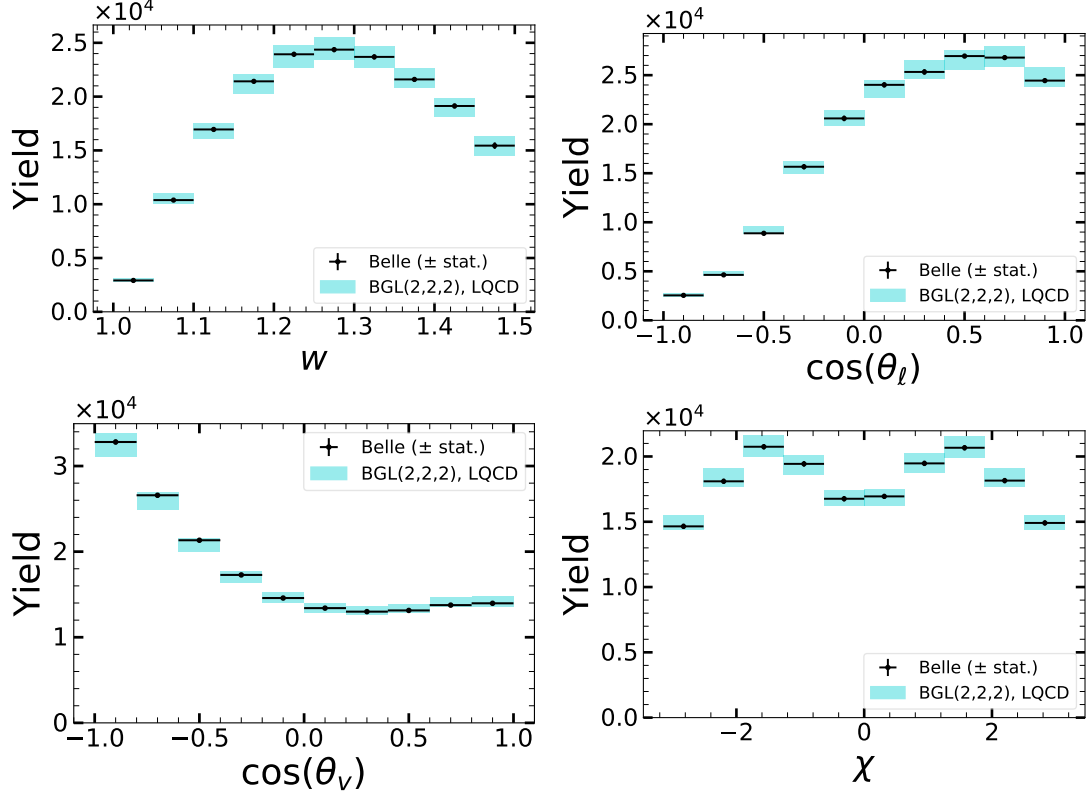


FIG. 5. The measured binned yields (data points) with statistical uncertainty for each observable of the $B^0 \rightarrow D^{*-} \ell^+ \nu_\ell$ decay overlaid with the BGL(2,2,2) (cyan) parametrization fit results where LQCD constraints have been introduced. The statistical and systematic uncertainties in the fits are determined in the same way as Fig. 1. The results from the fit are in agreement with the data.

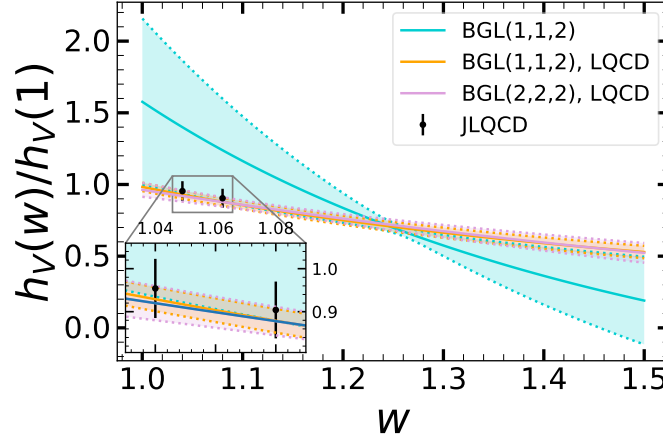


FIG. 6. The normalized form factor $h_V(w)/h_V(1)$ as a function of the hadronic recoil, w , for BGL(1,1,2) with (orange) and without (cyan) LQCD constraints, and BGL(2,2,2) with LQCD constraints (pink). The zoomed window within the plot is used to emphasize the region around the LQCD inputs for h_V . The central values and uncertainties are calculated via the same method as Fig. 3.

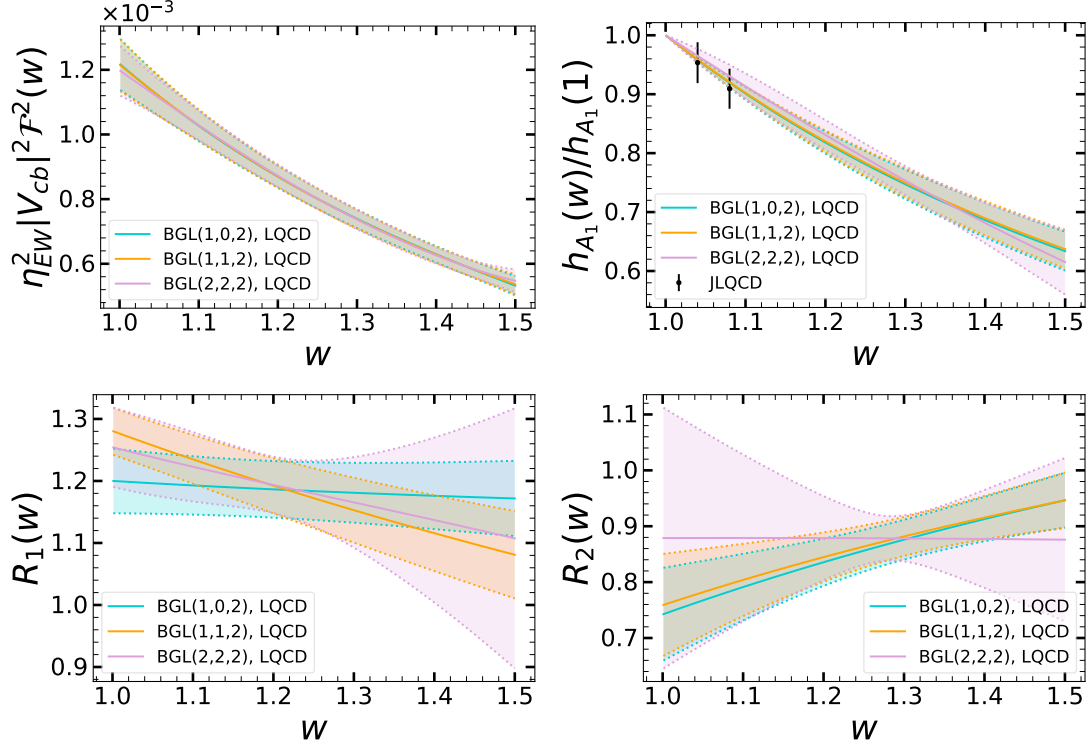


FIG. 7. The form factors and ratios $\eta_{EW}^2 |V_{cb}|^2 \mathcal{F}^2$, $h_{A_1}(w)/h_{A_1}(1)$, R_1 and R_2 as a function of the hadronic recoil, w , for BGL(1,0,2), BGL(1,1,2) and BGL(2,2,2) using preliminary input from JLQCD at non-zero recoil. The LQCD input has been included in the plot for h_{A_1} . The central values and uncertainties are calculated via the same method as Fig. 3.

TABLE VII. Correlations between the form factor values at non-zero recoil, $h_X(w)/h_X(1)$ where $X = A_1, V$ and $w = 1.04, 1.08$. The entries in this table are approximated from preliminary results from JLQCD. This correlation matrix is multiplied by the uncertainties for each LQCD point and then appended to the 40×40 statistical covariance matrix in a block-diagonal manner.

	$h_{A_1}(1.04)/h_{A_1}(1)$	$h_{A_1}(1.08)/h_{A_1}(1)$	$h_V(1.04)/h_V(1)$	$h_V(1.08)/h_V(1)$
$h_{A_1}(1.04)/h_{A_1}(1)$	1.0	0.85	0.38	0.49
$h_{A_1}(1.08)/h_{A_1}(1)$	0.85	1.0	0.18	0.44
$h_V(1.04)/h_V(1)$	0.38	0.18	1.0	0.93
$h_V(1.08)/h_V(1)$	0.49	0.44	0.93	1.0

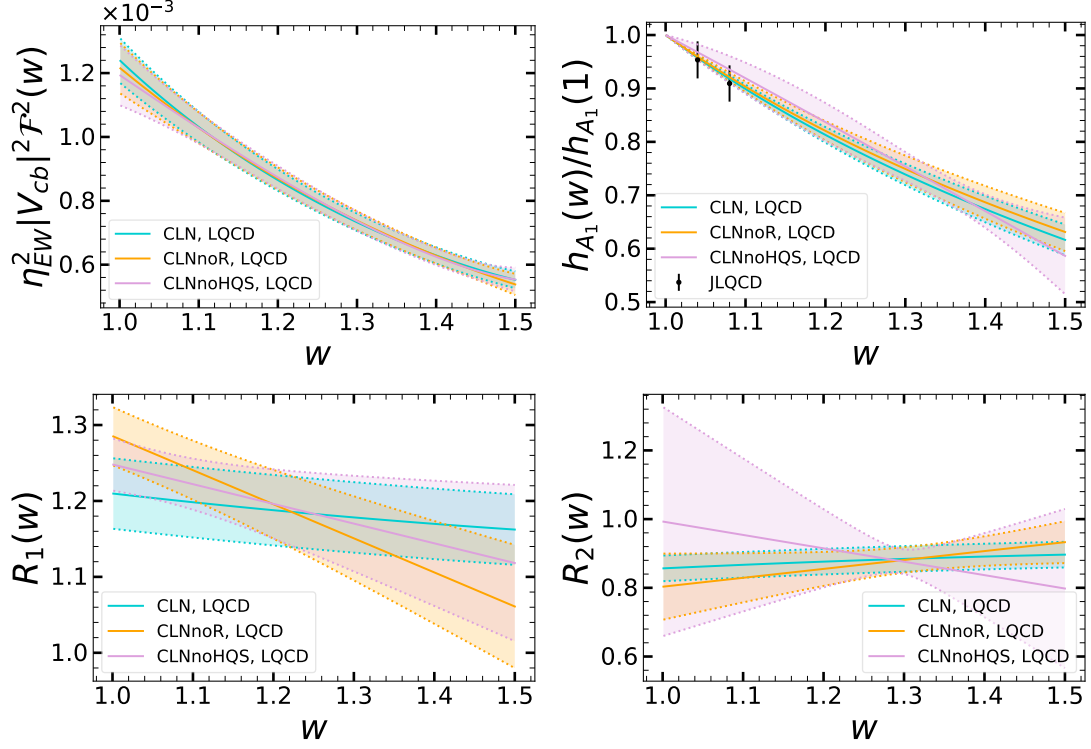


FIG. 8. The form factors and ratios $\eta_{EW}^2 |V_{cb}|^2 \mathcal{F}^2$, $h_{A_1}(w)/h_{A_1}(1)$, R_1 and R_2 as a function of the hadronic recoil, w , for CLN, CLNnoR and CLNnoHQS using preliminary input from JLQCD at non-zero recoil. The LQCD input has been included in the plot for h_{A_1} . The central values and uncertainties are calculated via the same method as Fig. 3.

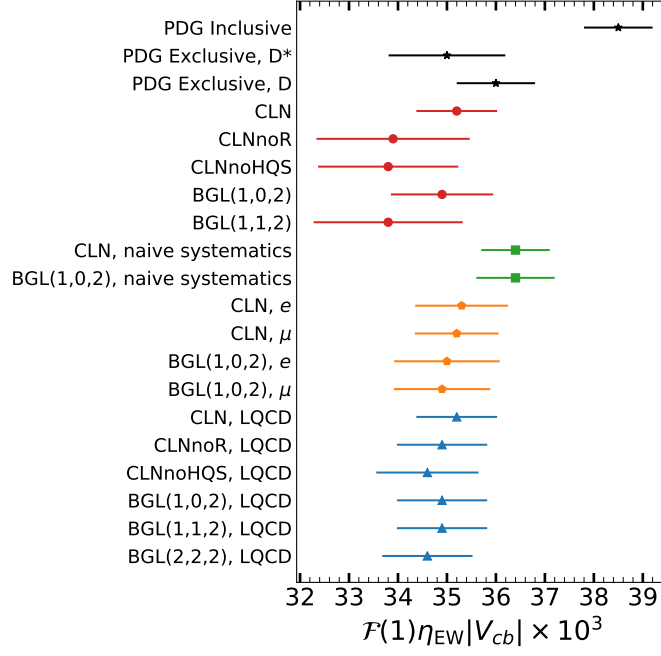


FIG. 9. Summary of the $\mathcal{F}(1)\eta_{EW}|V_{cb}|$ values from the various fit scenarios covered in this paper. For the PDG reference values we use $\mathcal{F}(1) = 0.904 \pm 0.012$.

Appendix A VERIFYING THE CHOLESKY DECOMPOSITION METHOD

When the systematic uncertainty from the Belle publication is added the covariance matrix, the minimizing function provides a biased fit due to high correlations, despite returning a lower χ^2 value. This causes a poor fit when compared to the results without this addition, as seen in the bias present in Fig. 10. Fit values for the free parameters with and without the addition of the systematic covariance matrix are listed in Table VIII and show inconsistency, particularly in the normalization. As the yield from the fit is determined in a forward-folding approach, this appears to have a reverse D’Agostini effect where the fit overestimates the yield and therefore also the $\mathcal{B}(B^0 \rightarrow D^{*-}\ell^+\nu_\ell)$ branching ratio and $\mathcal{F}(1)\eta_{EW}|V_{cb}|$.

To test the toy MC method with Cholesky decomposition for bias, the Belle analysis was repeated with a false data sample generated from arbitrarily chosen CLN parameters:

$$\begin{aligned}\rho^2 &= 1.1, \\ R_1(1) &= 1.2, \\ R_2(1) &= 0.8, \\ \eta_{EW}|V_{cb}| &= 0.04.\end{aligned}$$

The statistical uncertainties in each bin were defined as

the square root of the number of events in that bin while the statistical correlations were defined by the following:

$$\rho_{stat.}(i, j) = \begin{cases} 1 & i = j \\ 0.01 & i \neq j, i, j \text{ block diagonal} \\ 0 & \text{otherwise,} \end{cases} \quad (24)$$

where “ i, j block diagonal” refers to entries within the 10×10 sub-matrix for each observable along the diagonal of the full 40×40 statistical correlation matrix.

The systematic uncertainty is given by $\sigma_i = N_i^{exp}\epsilon_i$, where $\epsilon_i = 0.01$ in each bin and

$$\rho_{sys.}(i, j) = \begin{cases} 1 & i = j \\ 0.99 & \text{otherwise.} \end{cases} \quad (25)$$

The pull obtained from the fits from 10^4 iterations was measured, where the pull for the i^{th} fit, p_i , of each parameter measurement, x_i , is given by

$$p_{i,x} = \frac{x_i - \hat{x}}{\sigma_x}. \quad (26)$$

Here \hat{x} is the nominal value of the parameter, defined earlier, and $\sigma_x^2 = \sum_i (x_i - \hat{x})^2 / n$ for n fits. The results are found to have no bias, with the pull for each fit parameter being consistent with zero. Therefore, we consider this method of producing a toy MC sample via the Cholesky decomposition as suitable for determining the nominal values and uncertainties of parameters in the case of dominant scale errors with high correlations.

-
- [1] P. A. Zyla *et al.* (Particle Data Group), *Review of Particle Physics*, *Prog. Theor. Exp. Phys.* **2020** (2020).
 - [2] A. Sirlin, *Large $m(W)$, $m(Z)$ Behavior of the $O(\alpha)$ Corrections to Semileptonic Processes Mediated by W* , *Nucl. Phys. B* **196** (1982) 83–92.
 - [3] I. Caprini, L. Lellouch, and M. Neubert, *Dispersive bounds on the shape of $B \rightarrow D(*)\ell\nu$ form factors*, *Nucl. Phys. B* **530** (1998) 153–181.
 - [4] C. G. Boyd, B. Grinstein, and R. F. Lebed, *Precision corrections to dispersive bounds on form factors*, *Phys. Rev. D* **56** (1997) 6895–6911.
 - [5] E. Waheed, *et al.* (Belle Collaboration), *Measurement of the CKM matrix element $|V_{cb}|$ from $B^0 \rightarrow D^{*-}\ell^+\nu_\ell$ at Belle*, *Phys. Rev. D* **100** (2019) 052007.
 - [6] A. Abdesselam *et al.* (Belle Collaboration), *Precise determination of the CKM matrix element $|V_{cb}|$ with $B^0 \rightarrow D^{*+}\ell^-\bar{\nu}_\ell$ decays with hadronic tagging at Belle*, [arXiv:1702.01521](#).
 - [7] B. Grinstein and A. Kobach, *Model-Independent Extraction of $|V_{cb}|$ from $\bar{B} \rightarrow D^*\ell\bar{\nu}$* , *Phys. Lett. B* **771** (2017) 359–364 [[arXiv:1703.08170](#)].
 - [8] D. Bigi, P. Gambino, and S. Schacht, *A fresh look at the determination of $|V_{cb}|$ from $B \rightarrow D^*\ell\nu$* , *Phys. Lett. B* **769** (2017) 441–445 [[arXiv:1703.06124](#)].
 - [9] J. P. Lees *et al.* (BaBar Collaboration), *Extraction of form Factors from a Four-Dimensional Angular Analysis of $\bar{B} \rightarrow D^*\ell^-\bar{\nu}_\ell$* , *Phys. Rev. Lett.* **123** (2019) 091801 [[arXiv:1903.10002](#)].
 - [10] P. Gambino, M. Jung, and S. Schacht, *The V_{cb} puzzle: An update*, *Phys. Lett. B* **795** (2019) 386–390.
 - [11] F. U. Bernlochner, Z. Ligeti, and D. J. Robinson, *$N = 5, 6, 7, 8$: Nested hypothesis tests and truncation dependence of $|V_{cb}|$* , *Phys. Rev. D* **100** (2019) 013005 [[arXiv:1902.09553](#)].
 - [12] J. A. Bailey *et al.* (Fermilab Lattice, MILC Collaboration), *Update of $|V_{cb}|$ from the $\bar{B} \rightarrow D^*\ell\bar{\nu}$ form factor at zero recoil with three-flavor lattice QCD*, *Phys. Rev. D* **89** (2014) 114504 [[arXiv:1403.0635](#)].
 - [13] M. Tanabashi, *et al.* (Particle Data Group), *Review of Particle Physics*, *Phys. Rev. D* **98** (2018) 030001.
 - [14] G. D’Agostini, *On the use of the covariance matrix to fit correlated data*, *Nucl. Instrum. Methods A* **346** (1994) 306–311.
 - [15] A. Björck *et al.*, *Numerical Methods for Least Squares Problems*. Handbook of Numerical Analysis. Society for Industrial and Applied Mathematics, 1996.
 - [16] A. V. Waldron, M. D. Haigh, and A. Weber, *Combining Neutrino Oscillation Experiments with the Feldman-Cousins Method*, *New J. Phys.* **14** (2012) 063037 [[arXiv:1204.3450](#)].
 - [17] M. Jung and D. M. Straub, *Constraining new physics in $b \rightarrow c\ell\nu$ transitions*, *JHEP* **01** (2019) 009

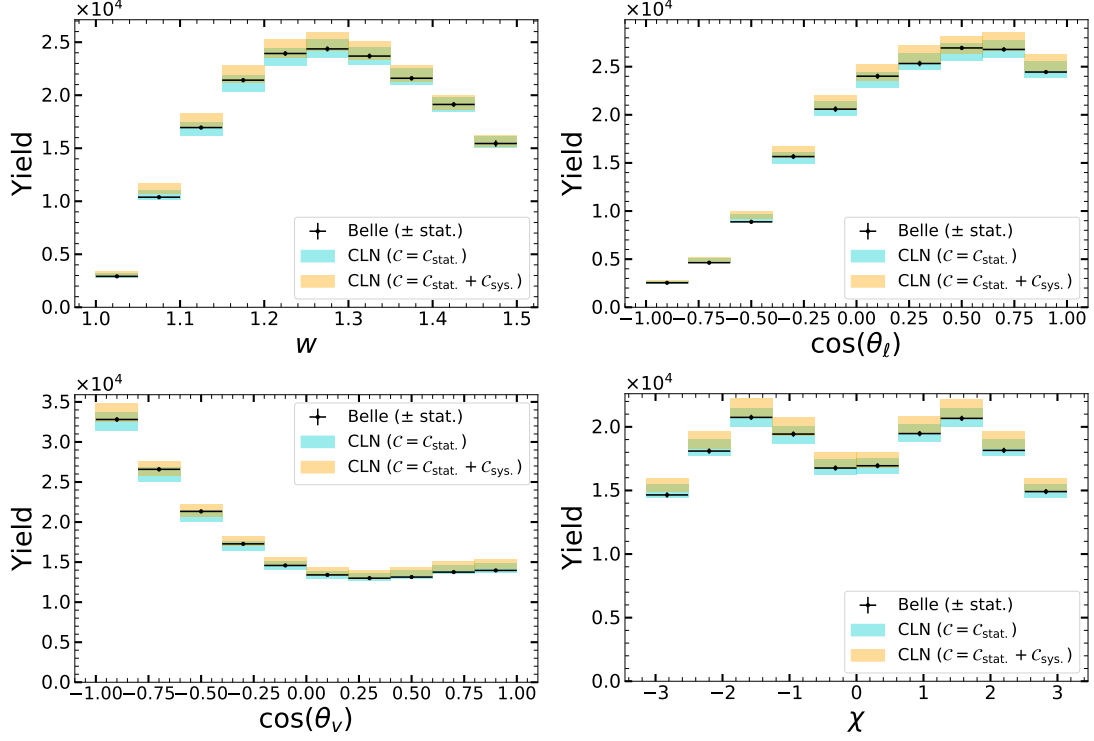


FIG. 10. (Appendix) The measured binned yields (data points) with statistical uncertainty for each observable of the $B^0 \rightarrow D^{*-} \ell^+ \nu_\ell$ decay overlaid with CLN fit results for different covariance matrices, \mathcal{C} , used in Eq. 14. Results are shown for the total covariance matrix being equal to the statistical covariance matrix alone (cyan), and the sum of both the statistical and systematic covariance matrices in a naive way (orange).

TABLE VIII. (Appendix) Fitted parameters in CLN and BGL(1,0,2) for combined electron and muon modes comparing different total covariance matrices. The results with only statistical uncertainties are obtained by setting \mathcal{C} from Eq. 14 to be equal to $\mathcal{C}_{\text{stat.}}$ and the results from combining statistical and systematic uncertainties in a naive way are obtained using $\mathcal{C} = \mathcal{C}_{\text{stat.}} + \mathcal{C}_{\text{sys.}}$. The branching ratio is obtained from the fit and $\mathcal{F}(1)\eta_{\text{EW}}|V_{cb}|$ is calculated from Eq. 13.

Covariance:	stat.	sys.+stat.
CLN		
ρ^2	1.09 ± 0.04	1.16 ± 0.04
$R_1(1)$	1.20 ± 0.03	1.18 ± 0.04
$R_2(1)$	0.86 ± 0.02	0.85 ± 0.03
$\mathcal{F}(1)\eta_{\text{EW}} V_{cb} \times 10^3$	35.3 ± 0.2	36.4 ± 0.7
$\mathcal{B}(B^0 \rightarrow D^{*-} \ell^+ \nu_\ell)$	4.93%	5.09%
χ^2/ndf	41/36	24/36
BGL(1,0,2)		
$\tilde{a}_0^f \times 10^3$	0.506 ± 0.004	0.53 ± 0.01
$\tilde{a}_1^f \times 10^3$	0.6 ± 0.2	0.2 ± 0.3
$\tilde{a}_1^{F_1} \times 10^3$	0.30 ± 0.07	0.2 ± 0.1
$\tilde{a}_2^{F_1} \times 10^3$	-3.8 ± 1.4	-2.6 ± 1.8
$\tilde{a}_0^g \times 10^3$	0.92 ± 0.02	0.92 ± 0.03
$\mathcal{F}(1)\eta_{\text{EW}} V_{cb} \times 10^3$	34.9 ± 0.3	36.4 ± 0.8
$\mathcal{B}(B^0 \rightarrow D^{*-} \ell^+ \nu_\ell)$	4.93%	5.09%
χ^2/ndf	39/35	24/35

- [arXiv:1801.01112].
- [18] N. Isgur and M. B. Wise, *Weak decays of heavy mesons in the static quark approximation*, *Phys. Lett. B* **232** (1989) 113–117.
 - [19] N. Isgur and M. B. Wise, *Weak transition form factors between heavy mesons*, *Phys. Lett. B* **237** (1990) 527–530.
 - [20] F. U. Bernlochner, Z. Ligeti, M. Papucci, and D. J. Robinson, *Tensions and correlations in $|V_{cb}|$ determinations*, *Phys. Rev. D* **96** (2017) 091503 [arXiv:1708.07134].
 - [21] T. Kaneko, *et al.* (JLQCD Collaboration) in *37th International Symposium on Lattice Field Theory*. 2019.
 - [22] A. Vaquero, *et al.*, $\overline{B} \rightarrow D^* \ell \overline{\nu}$ at Non-Zero Recoil, *EPJ Web Conf.* **175** (2018) 13003 [arXiv:1710.09817].
 - [23] A. Vaquero, *et al.* in *17th Conference on Flavor Physics and CP Violation*. 2019. arXiv:1906.01019.
 - [24] S. Jaiswal, S. Nandi, and S. K. Patra, *Updates on extraction of $|V_{cb}|$ and SM prediction of $R(D^*)$ in $B \rightarrow D^* \ell \nu_\ell$ decays*, *JHEP* **06** (2020) 165 [arXiv:2002.05726].
 - [25] S. Jaiswal, S. Nandi, and S. K. Patra, *Extraction of $|V_{cb}|$ from $B \rightarrow D^{(*)} \ell \nu_\ell$ and the Standard Model predictions of $R(D^{(*)})$* , *JHEP* **12** (2017) 060 [arXiv:1707.09977].